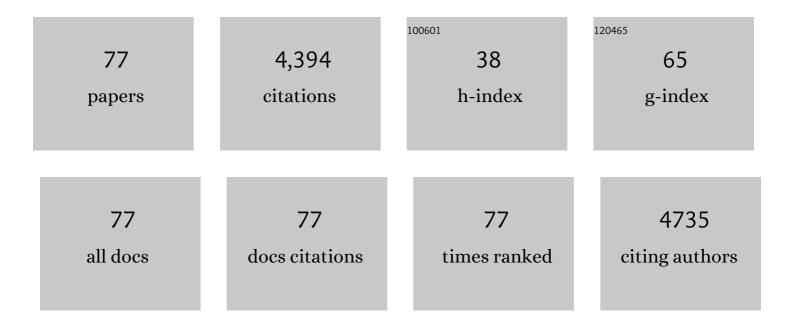
Christopher A Gorski

List of Publications by Year in descending order

Source: https://exaly.com/author-pdf/4963636/publications.pdf Version: 2024-02-01



#	Article	IF	CITATIONS
1	Co-precipitation synthesis control for sodium ion adsorption capacity and cycle life of copper hexacyanoferrate electrodes in battery electrode deionization. Chemical Engineering Journal, 2022, 435, 135001.	6.6	8
2	Power and energy capacity tradeoffs in an all-aqueous copper thermally regenerative ammonia battery. Journal of Power Sources, 2022, 531, 231339.	4.0	13
3	Thermodynamic and Kinetic Analyses of Ion Intercalation/Deintercalation Using Different Temperatures on NiHCF Electrodes for Battery Electrode Deionization. Environmental Science & Technology, 2022, 56, 8932-8941.	4.6	9
4	Optimizing Electrodeposited Manganese Oxide at Carbon Cloth Electrodes for Harvesting Salinity-Gradient Energy. Journal of the Electrochemical Society, 2021, 168, 024505.	1.3	5
5	Metal-Ion Depletion Impacts the Stability and Performance of Battery Electrode Deionization over Multiple Cycles. Environmental Science & Technology, 2021, 55, 5412-5421.	4.6	24
6	Electrochemically Mediated CO ₂ Capture Using Aqueous Cu(II)/Cu(I) Imidazole Complexes. ACS ES&T Engineering, 2021, 1, 1084-1093.	3.7	6
7	An All-Aqueous Thermally Regenerative Ammonia Battery Chemistry Using Cu(I, II) Redox Reactions. Journal of the Electrochemical Society, 2021, 168, 070523.	1.3	16
8	Effects of Fe(III) Oxide Mineralogy and Phosphate on Fe(II) Secondary Mineral Formation during Microbial Iron Reduction. Minerals (Basel, Switzerland), 2021, 11, 149.	0.8	19
9	Using a vapor-fed anode and saline catholyte to manage ion transport in a proton exchange membrane electrolyzer. Energy and Environmental Science, 2021, 14, 6041-6049.	15.6	22
10	Influence of Hydrotropes on the Solubilities and Diffusivities of Redox-Active Organic Compounds for Aqueous Flow Batteries. ACS Omega, 2021, 6, 30800-30810.	1.6	11
11	Role of Carbonate in Thermodynamic Relationships Describing Pollutant Reduction Kinetics by Iron Oxide-Bound Fe ²⁺ . Environmental Science & Technology, 2020, 54, 10109-10117.	4.6	10
12	Using reverse osmosis membranes to control ion transport during water electrolysis. Energy and Environmental Science, 2020, 13, 3138-3148.	15.6	49
13	Recovery of ammonium and phosphate using battery deionization in a background electrolyte. Environmental Science: Water Research and Technology, 2020, 6, 1688-1696.	1.2	13
14	Few-Layer Clayenes for Material and Environmental Applications. ACS Applied Materials & Interfaces, 2020, 12, 11171-11179.	4.0	5
15	Improving the Thermodynamic Energy Efficiency of Battery Electrode Deionization Using Flow-Through Electrodes. Environmental Science & Technology, 2020, 54, 3628-3635.	4.6	32
16	Electrochemical Desalination Using Intercalating Electrode Materials: A Comparison of Energy Demands. Environmental Science & amp; Technology, 2020, 54, 3653-3662.	4.6	47
17	Surveying Manganese Oxides as Electrode Materials for Harnessing Salinity Gradient Energy. Environmental Science & Technology, 2020, 54, 5746-5754.	4.6	17
18	Stepwise ammonium enrichment using selective battery electrodes. Environmental Science: Water Research and Technology, 2020, 6, 1649-1657.	1.2	8

4.0

74

#	Article	IF	CITATIONS
19	Influence of Ligands on the Cu(I/II) Redox Reaction for Redox Flow Batteries. ECS Meeting Abstracts, 2020, MA2020-01, 510-510.	0.0	0
20	Electron Donor Utilization and Secondary Mineral Formation during the Bioreduction of Lepidocrocite by Shewanella putrefaciens CN32. Minerals (Basel, Switzerland), 2019, 9, 434.	0.8	18
21	Electro-Forward Osmosis. Environmental Science & amp; Technology, 2019, 53, 8352-8361.	4.6	16
22	Quantifying Ca exchange in gypsum using a 45Ca tracer: Implications for interpreting Ca isotopic effects in experimental and natural systems. Geochimica Et Cosmochimica Acta, 2019, 259, 371-390.	1.6	5
23	Low temperature stable mineral recrystallization of foraminiferal tests and implications for the fidelity of geochemical proxies. Earth and Planetary Science Letters, 2019, 506, 428-440.	1.8	29
24	A biochemical framework for anaerobic oxidation of methane driven by Fe(III)-dependent respiration. Nature Communications, 2018, 9, 1642.	5.8	88
25	Emerging electrochemical and membrane-based systems to convert low-grade heat to electricity. Energy and Environmental Science, 2018, 11, 276-285.	15.6	172
26	Linking Thermodynamics to Pollutant Reduction Kinetics by Fe ²⁺ Bound to Iron Oxides. Environmental Science & Technology, 2018, 52, 5600-5609.	4.6	59
27	Mediated Electrochemical Reduction of Iron (Oxyhydr-)Oxides under Defined Thermodynamic Boundary Conditions. Environmental Science & Technology, 2018, 52, 560-570.	4.6	35
28	Chemical Degradation of Polyacrylamide during Hydraulic Fracturing. Environmental Science & Technology, 2018, 52, 327-336.	4.6	68
29	A thermally regenerative ammonia battery with carbon-silver electrodes for converting low-grade waste heat to electricity. Journal of Power Sources, 2018, 373, 95-102.	4.0	79
30	Ammonium Removal from Domestic Wastewater Using Selective Battery Electrodes. Environmental Science and Technology Letters, 2018, 5, 578-583.	3.9	77
31	Rationally Selecting Manganese Oxide Electrodes for Salinity Gradient Energy Production. ECS Meeting Abstracts, 2018, , .	0.0	0
32	Improved electrical power production of thermally regenerative batteries using a poly(phenylene) Tj ETQq0 0 0 rg	BT /Overlo 4.0	ock 10 Tf 50
33	Redox controls on arsenic enrichment and release from aquifer sediments in central Yangtze River Basin. Geochimica Et Cosmochimica Acta, 2017, 204, 104-119.	1.6	101
34	A pH-Gradient Flow Cell for Converting Waste CO ₂ into Electricity. Environmental Science and Technology Letters, 2017, 4, 49-53.	3.9	25
35	Integrating Reverseâ€Electrodialysis Stacks with Flow Batteries for Improved Energy Recovery from Salinity Gradients and Energy Storage. ChemSusChem, 2017, 10, 797-803.	3.6	28

³⁶ Electrical power production from low-grade waste heat using a thermally regenerative ethylenediamine battery. Journal of Power Sources, 2017, 351, 45-50.

Christopher A Gorski

#	Article	IF	CITATIONS
37	High power densities created from salinity differences by combining electrode and Donnan potentials in a concentration flow cell. Energy and Environmental Science, 2017, 10, 1003-1012.	15.6	55
38	Susceptibility of Goethite to Fe ²⁺ -Catalyzed Recrystallization over Time. Environmental Science & amp; Technology, 2017, 51, 11681-11691.	4.6	37
39	Low Energy Desalination Using Battery Electrode Deionization. Environmental Science and Technology Letters, 2017, 4, 444-449.	3.9	224
40	Stable mineral recrystallization in low temperature aqueous systems: A critical review. Geochimica Et Cosmochimica Acta, 2017, 198, 439-465.	1.6	84
41	Removal of copper from water using a thermally regenerative electrodeposition battery. Journal of Hazardous Materials, 2017, 322, 551-556.	6.5	67
42	A Flavin-Based pH Flow Battery That Recharges with Waste Heat or Carbon Dioxide Emissions. ECS Meeting Abstracts, 2017, , .	0.0	0
43	A Fully Regenerable Thermal Silver Ammonia Battery to Convert Low-Grade Waste Heat to Electricity. ECS Meeting Abstracts, 2017, , .	0.0	0
44	High Electrical Power Densities from Salinity Gradients By Combining Electrode and Donnan Potentials in a Single Electrochemical Cell. ECS Meeting Abstracts, 2017, , .	0.0	0
45	Integrating Reverse-Electrodialysis Stacks with Flow Batteries to Achieve Improved Energy Recovery from Salinity Gradients and Energy Storage. ECS Meeting Abstracts, 2017, , .	0.0	0
46	Water Desalination By Pseudocapacitive Deionization. ECS Meeting Abstracts, 2017, , .	0.0	0
47	A Thermallyâ€Regenerative Ammoniaâ€Based Flow Battery for Electrical Energy Recovery from Waste Heat. ChemSusChem, 2016, 9, 873-879.	3.6	94
48	Anisotropic Morphological Changes in Goethite during Fe ²⁺ -Catalyzed Recrystallization. Environmental Science & Technology, 2016, 50, 7315-7324.	4.6	55
49	Harvesting Energy from Salinity Differences Using Battery Electrodes in a Concentration Flow Cell. Environmental Science & Technology, 2016, 50, 9791-9797.	4.6	67
50	The role of dissolved Fe(II) concentration in the mineralogical evolution of Fe (hydr)oxides during redox cycling. Chemical Geology, 2016, 438, 163-170.	1.4	41
51	Thermodynamic Characterization of Iron Oxide–Aqueous Fe ²⁺ Redox Couples. Environmental Science & Technology, 2016, 50, 8538-8547.	4.6	106
52	Self-Generated Electrokinetic Fluid Flows during Pseudomorphic Mineral Replacement Reactions. Langmuir, 2016, 32, 5233-5240.	1.6	13
53	Evaluating Batteryâ€like Reactions to Harvest Energy from Salinity Differences using Ammonium Bicarbonate Salt Solutions. ChemSusChem, 2016, 9, 981-988.	3.6	36
54	Interactions Between Fe(III)-Oxides and Fe(III)-Phyllosilicates During Microbial Reduction 1: Synthetic Sediments. Geomicrobiology Journal, 2016, 33, 793-806.	1.0	7

#	Article	IF	CITATIONS
55	lron(III)-Bearing Clay Minerals Enhance Bioreduction of Nitrobenzene by <i>Shewanella putrefaciens</i> CN32. Environmental Science & Technology, 2015, 49, 1418-1426.	4.6	71
56	Linear Free Energy Relationships for the Biotic and Abiotic Reduction of Nitroaromatic Compounds. Environmental Science & Technology, 2015, 49, 3557-3565.	4.6	34
57	Electrochemical Analyses of Redox-Active Iron Minerals: A Review of Nonmediated and Mediated Approaches. Environmental Science & Technology, 2015, 49, 5862-5878.	4.6	120
58	Effects of Phosphate on Secondary Mineral Formation During the Bioreduction of Akaganeite (.β-FeOOH): Green Rust Versus Framboidal Magnetite. Current Inorganic Chemistry, 2015, 5, 214-224.	0.2	19
59	Fe(II) Uptake on Natural Montmorillonites. I. Macroscopic and Spectroscopic Characterization. Environmental Science & Technology, 2014, 48, 8688-8697.	4.6	41
60	Thermodynamic Controls on the Microbial Reduction of Iron-Bearing Nontronite and Uranium. Environmental Science & Technology, 2014, 48, 2750-2758.	4.6	38
61	Redox Properties of Structural Fe in Clay Minerals: 3. Relationships between Smectite Redox and Structural Properties. Environmental Science & Technology, 2013, 47, 13477-13485.	4.6	131
62	Effects of Bound Phosphate on the Bioreduction of Lepidocrocite (γ-FeOOH) and Maghemite (γ-Fe ₂ O ₃) and Formation of Secondary Minerals. Environmental Science & Technology, 2013, 47, 9157-9166.	4.6	73
63	Influence of Fe2+-catalysed iron oxide recrystallization on metal cycling. Biochemical Society Transactions, 2012, 40, 1191-1197.	1.6	80
64	Redox Properties of Structural Fe in Clay Minerals. 1. Electrochemical Quantification of Electron-Donating and -Accepting Capacities of Smectites. Environmental Science & Technology, 2012, 46, 9360-9368.	4.6	125
65	Coal Fly Ash as a Source of Iron in Atmospheric Dust. Environmental Science & Technology, 2012, 46, 2112-2120.	4.6	129
66	Fe Atom Exchange between Aqueous Fe ²⁺ and Magnetite. Environmental Science & Technology, 2012, 46, 12399-12407.	4.6	112
67	Thermodynamics of the magnetite-ulvospinel (Fe3O4-Fe2TiO4) solid solution. American Mineralogist, 2012, 97, 1330-1338.	0.9	45
68	Redox Properties of Structural Fe in Clay Minerals. 2. Electrochemical and Spectroscopic Characterization of Electron Transfer Irreversibility in Ferruginous Smectite, SWa-1. Environmental Science & Technology, 2012, 46, 9369-9377.	4.6	115
69	Influence of Magnetite Stoichiometry on U ^{VI} Reduction. Environmental Science & Technology, 2012, 46, 778-786.	4.6	128
70	Fe ²⁺ Sorption at the Fe Oxide-Water Interface: A Revised Conceptual Framework. ACS Symposium Series, 2011, , 315-343.	0.5	66
71	Spectroscopic Evidence for Interfacial Fe(II)â^Fe(III) Electron Transfer in a Clay Mineral. Environmental Science & Technology, 2011, 45, 540-545.	4.6	141
72	Assessing the redox properties of iron-bearing clay minerals using homogeneous electrocatalysis. Applied Geochemistry, 2011, 26, S191-S193.	1.4	6

#	Article	IF	CITATIONS
73	Determination of nanoparticulate magnetite stoichiometry by Mossbauer spectroscopy, acidic dissolution, and powder X-ray diffraction: A critical review. American Mineralogist, 2010, 95, 1017-1026.	0.9	207
74	Effects of Oxyanions, Natural Organic Matter, and Bacterial Cell Numbers on the Bioreduction of Lepidocrocite (γ-FeOOH) and the Formation of Secondary Mineralization Products. Environmental Science & Technology, 2010, 44, 4570-4576.	4.6	125
75	Connecting Observations of Hematite (α-Fe ₂ O ₃) Growth Catalyzed by Fe(II). Environmental Science & Technology, 2010, 44, 61-67.	4.6	110
76	Redox Behavior of Magnetite: Implications for Contaminant Reduction. Environmental Science & Technology, 2010, 44, 55-60.	4.6	195
77	Influence of Magnetite Stoichiometry on Fe ^{II} Uptake and Nitrobenzene Reduction. Environmental Science & Technology, 2009, 43, 3675-3680.	4.6	149